



Evidence for Genuine Hydrogen Bonding in Gold(I) Complexes

Mathilde Rigoulet, Stephane Massou, E. Daiann Sosa Carrizo, Sonia Mallet-Ladeira, Abderrahmane Amgoune, Karinne Miqueu, Didier Bourissou

► To cite this version:

Mathilde Rigoulet, Stephane Massou, E. Daiann Sosa Carrizo, Sonia Mallet-Ladeira, Abderrahmane Amgoune, et al.. Evidence for Genuine Hydrogen Bonding in Gold(I) Complexes. Proceedings of the National Academy of Sciences of the United States of America, 2019, 116 (1), pp.46-51. 10.1073/pnas.1817194116 . hal-02398808

HAL Id: hal-02398808

<https://hal.science/hal-02398808v1>

Submitted on 8 Dec 2019

HAL is a multi-disciplinary open access archive for the deposit and dissemination of scientific research documents, whether they are published or not. The documents may come from teaching and research institutions in France or abroad, or from public or private research centers.

L'archive ouverte pluridisciplinaire **HAL**, est destinée au dépôt et à la diffusion de documents scientifiques de niveau recherche, publiés ou non, émanant des établissements d'enseignement et de recherche français ou étrangers, des laboratoires publics ou privés.

Evidence for Genuine Hydrogen Bonding in Gold(I) Complexes

Mathilde Rigoulet^a, Stéphane Massou^b, E. Daiann Sosa Carrizo^c, Sonia Mallet-Ladeira^b,
Abderrahmane Amgoune^a, Karinne Miqueu^c, and Didier Bourissou^{a,1}

^aLaboratoire Hétérochimie Fondamentale et Appliquée (LHFA, UMR 5069), 118 Route de Narbonne,
31062 Toulouse Cedex 09, France;

^bInstitut de Chimie de Toulouse (ICT, FR 2599), 118 Route de Narbonne, 31062 Toulouse Cedex 09,
France;

^cCNRS/UNIV PAU & PAYS ADOUR, Institut des Sciences Analytiques et de Physico-Chimie pour
l'Environnement et les Matériaux (IPREM, UMR 5254), Hélioparc, 2 Avenue du Président Angot,
64053 Pau Cedex 09, France.

¹To whom correspondence should be addressed. Email: dbouriss@chimie.ups-tlse.fr

Keywords: gold / hydrogen bonding / non-covalent interactions / relativistic effects

Abstract:

The ability of gold to act as proton acceptor and participate in hydrogen bonding remains an open question. Here we report the synthesis and characterization of cationic gold(I) complexes featuring ditopic phosphine-ammonium (P,NH⁺) ligands. Besides the presence of short Au...H contacts in the solid state, the presence of Au...H–N hydrogen bonds has been inferred by NMR and IR spectroscopies. The bonding situation has been extensively analysed computationally. All features are consistent with the presence of 3-center 4-electron attractive interactions combining electrostatic and orbital components. The role of relativistic effects has been examined and the analysis has been extended to other recently described gold(I) complexes.

Introduction

Hydrogen bonds are ubiquitous and play a major role in chemistry. Besides the classical hydrogen-bond acceptors (namely N, O, the halogens, S and P), transition metals have been recognized to also participate in hydrogen bonding towards protonic H–X fragments. Since the 1990s, such $M\cdots H-X$ interactions have garnered great interest (1, 2). Numerous studies have been carried out to better understand this unusual bonding situation, to delineate the influence of $M\cdots H-X$ interactions on the structure and properties of transition metal complexes. It is also of note that $M\cdots H-X$ interactions are relevant to the protonation of transition metals to form metal hydrides (1, 3, 4). $M\cdots H-X$ interactions have been unambiguously authenticated both intra- and intermolecularly with various hydrogen bond donor moieties (ammoniums, amides, water...) and electron-rich transition metals (mainly Pt and Co).

The case of gold is very singular and deserves special attention. Due to strong relativistic effects (5, 6), gold displays very different properties than the other transition metals. It is a very peculiar element among the d-block of the periodic table that has attracted considerable interest over the last 2-3 decades due to its recently discovered and unique efficiency in catalysis (7–11), both heterogeneous and homogeneous. Considerable efforts have also been involved in better understanding the structure and reactivity of gold compounds. In this respect, it is striking to note that the ability of gold to participate in hydrogen bonding still remains an open question, despite intense experimental and theoretical research in the last 12 years. The most relevant contributions in the field will be briefly presented hereafter. For a comprehensive and authoritative state-of-the-art, the reader is invited to refer to the review published in 2014 by Schmidbaur *et al* (12).

In the mid 2000's, Jansen prepared and characterized by X-ray diffraction (XRD) an ammonia complex of the auride ion Au^- . The presence of $Au\cdots H-N$ hydrogen bonding was inferred based on the relatively short $Au\cdots H$ distance (2.58(1) Å) and wide $Au\cdots H-N$ angle (158(1)°) (13). A number of Au(I) and Au(III) complexes were also reported to display relatively short $Au\cdots H$ distances in the solid state (2.3–3.0 Å), but the precise location of H atoms in close proximity of such an heavy element as gold by X-ray diffraction is intrinsically challenging (14). As emphasized in the review by Schmidbaur *et al* (12), the observed $Au\cdots H$ contacts are likely to result from other factors than hydrogen bonding (cation/anion interactions, crystal packing...) and their attractive nature has not been substantiated. Last year, the existence of $Au\cdots H-C$ interactions akin to hydrogen bonds (15–17) within divalent hexagold clusters stabilized by diphosphine ligands was discussed by Konishi *et al* (18) based on the short $Au\cdots H-C$ contacts observed by X-ray diffraction (2.62 Å) and on the substantial downfield shift of the corresponding 1H and ^{13}C NMR signals. Kryachko *et al* have performed early on computational studies on $Au\cdots H-X$ ($X = N, O, F$) hydrogen bonds in gold complexes and clusters (19–21). In addition, recent theoretical studies combining geometry optimisations and bonding analyses have examined and supported the possible existence of $Au\cdots H-X$ hydrogen bonding in Au(I) molecular complexes, stimulating and providing guidelines for forthcoming experimental studies: Esterhuysen *et al* investigated extensively the interaction between anionic divalent gold(I) complexes and water (22, 23), while Berger, Monkowius *et al* performed a detailed study on a neutral gold(I) complex with a chelated NH-pyridinium moiety (24).

The absence of compelling evidence for hydrogen bonding involving gold is widely recognized and well summarized by the following statements excerpted from recent authoritative contributions:

- "A screening of the literature on gold compounds in which the gold atoms may be involved in intra- and intermolecular hydrogen bonding has not produced consistent evidence for any major influences of interactions of the type $\text{Au}\cdots\text{H}-\text{X}$ on the molecular structure and dynamics of the systems concerned." (Schmidbaur *et al*, 2014)(12)
- " $\text{Au}\cdots\text{H}$ interactions, particularly in complexes, cannot be discussed with confidence as yet" (Esterhuysen *et al*, 2016)(22)
- "While certain classes of H-bonds to Au(I) coordination centers have been proposed (...) on the basis of quantum chemical calculations (...), evidence from the experimental side is sparse at most and even the principal possibility of effective $\text{Au}\cdots\text{H}$ hydrogen bonds is set into question" (Berger, Monkowius *et al*, 2017)(24)
- "even now there are no examples of spectroscopically identified "hydrogen-bond type" $\text{Au}\cdots\text{H}$ interactions." (Konishi *et al*, 2017)(18).

Two main challenges must be overcome to establish and authenticate hydrogen bonding in gold complexes. On the one hand, the inherently weak $\text{Au}\cdots\text{H}-\text{X}$ interaction must be favoured over other competitive bonding situations such as intermolecular $\text{Au}\cdots\text{Au}$ aurophilic interactions (25) and/or hydrogen bonding of the $\text{H}-\text{X}$ moiety with electron-rich sites of the ligands surrounding the metal (26). On the other hand, conspicuous evidence for the existence of the $\text{Au}\cdots\text{H}-\text{X}$ bond should be obtained, besides the observation of short $\text{Au}\cdots\text{H}$ contacts in XRD analysis.

Based on recent developments in gold chemistry, we reasoned that (P,N) ligands such as *ortho*-amino phenylphosphines (DalPhos) may be good candidates and give access to hydrogen-bonded complexes (Fig. 1). The hemilabile character of the DalPhos ligands has been shown by L. Zhang *et al* to efficiently temper the reactivity of α -oxocarbenes (27–32). In addition, our group recently demonstrated the feasibility and easiness of oxidative addition to gold thanks to such (P,N) ligands (the hard N center stabilizes the Au(III) product and lowers the activation barrier) providing a new pathway for Au(I)/Au(III) catalysis (33). Due to its basic character, the nitrogen center also gives the opportunity to form an ammonium with a protonic N–H bond in close proximity to gold(I). As reported hereafter, this strategy proved fruitful and enabled us to form and authenticate hydrogen-bonded gold(I) complexes. It is worthwhile to note the structural analogy existing between the target compounds and the Au complexes deriving from (P,B) and (P,Al) ambiphilic ligands we reported previously, in which the Lewis acid moiety coordinates as a σ -acceptor Z-type ligand with Au acting as a Lewis base (34–36).

<Fig. 1>

Results and Discussion

Synthesis and characterization of the cationic gold complex 2.

Addition of 1 equivalent of trifluoromethane sulfonic acid (HOTf) to the MeDalPhos gold complex **1** immediately leads to a new complex **2** according to ^{31}P NMR spectroscopy (Scheme 1) and ^1H NMR unambiguously indicates protonation of the nitrogen atom. A broad N–H signal appears at δ 10.9 ppm while the $\text{N}(\text{CH}_3)_2$ signal is shifted to low field by about 1 ppm and resonates as a doublet with a $^3J(\text{H}-\text{H})$ coupling constant of 5.0 Hz. Of note, complex **2** can also be prepared by protonating the (P,N) ligand **3** prior to coordination to gold. Upon addition of HOTf, the phosphorus atom, not the nitrogen, is protonated, and the P–H phosphonium salt **4** is obtained. Diagnostic NMR features are

the low-field shift of the ^{31}P NMR signal (δ 17.5 ppm), the large $^1\text{J}(\text{P-H})$ coupling constant (485.3 Hz) and the absence of low-field shift of the $\text{N}(\text{CH}_3)_2$ ^1H NMR signal. As shown by X-ray diffraction (*SI Appendix*), the same tautomer is present in the solid state. Despite the protonation of phosphorus, compound **4** reacts rapidly with $\text{AuCl}(\text{SMe}_2)$ to give complex **2**. The proton shifts from P to N and the P atom coordinates to gold, displacing the SMe_2 ligand. DFT Calculations predict that protonation of the P atom of **3** is slightly more favoured thermodynamically ($\Delta G = 1.6$ kcal/mol) than that of the N atom, and that the activation barrier for the proton shift from P to N is fairly accessible at room temperature ($\Delta G^\ddagger = 7.7$ kcal/mol) (*SI Appendix*).

<Scheme 1>

Crystals of **2** were grown from a dichloromethane/pentane solution at -30°C and analysed by X-ray diffraction (*SI Appendix*). The H atom at N was located in the difference Fourier map and refined freely. There is no interaction between the acidic proton at N and the TfO^- counteranion (shortest distance > 4.4 Å), compound **2** adopts a separated ion-pair structure. The N-H bond points towards Au and the $\text{N-H}\cdots\text{Au}$ skeleton is close to linear ($165(2)^\circ$). The $\text{Au}\cdots\text{H}$ distance ($2.24(3)$ Å) is well within the sum of van der Waals radii (2.86 Å) (37) and falls in the very low range of those previously reported (12). As pointed out previously, short $\text{N-H}\cdots\text{Au}$ contacts are not indicative of attractive interactions and the associated metrical parameters should be considered with caution (14).

Multi-nuclear NMR confirms the general connectivity and according to 2D ^1H - ^1H NOESY experiments, complex **2** adopts in solution the same conformation than in the solid state (the Ad groups at P and the Me groups at N show correlations with the adjacent H atoms of the *ortho*-phenylene spacer). The very high ^1H NMR chemical shift of the N-H proton (10.9 ppm) is typical of H-bonding (1, 2, 38). Spin-spin coupling has also been inferred as a characteristic of H-bonding $\text{M}\rightarrow\text{H-X}$ interactions, although such couplings have been measured only very rarely. The $^1\text{J}(\text{N-H})$ coupling in complex **2** was determined precisely at natural ^{15}N abundance *via* a ^1H - ^{15}N HSQC experiment using homonuclear band selective (HOBS) detection scheme (*SI Appendix*). The obtained value (69.7 Hz) is very close to that reported by Pregosin and van Koten for a Pt(II) complex featuring an intramolecularly hydrogen-bonded NMe_2H^+ moiety (39, 40).

Infrared spectroscopy can also be a useful analytical probe. For example, significant decrease of the O-H stretching frequency was reported for the H-bonding of perfluoroalcohols H-ORf to Co, Rh and Ir (3). Recent computational studies suggest that gold may follow a similar trend (24, 41). No characteristic band was detected for the N-H stretch of **2**. Considering it may be masked by the C-H stretches, we turned to the deuterium-labeled complex **2-D** which was readily prepared using DOTf (*SI Appendix*). A N-D band appeared at 2124 cm^{-1} in the IR spectrum, corresponding to a N-H stretch at about 3000 cm^{-1} . This is 500 cm^{-1} lower than typical wavenumbers for free N-H (ammonium) oscillators. This shift confirms the presence of $\text{Au}\cdots\text{H-N}$ bonding in solution and provides direct spectroscopic evidence for such H-bonding.

To probe the chemical influence of the $\text{Au}\cdots\text{H-N}$ interaction in complex **2**, we then examined the possibility of proton transfer. Mixing the neutral gold(I) complex **1** with its protonated form **2** in solution give two well-resolved ^{31}P NMR signals at room temperature, indicating slow, if any, proton transfer and chemical exchange between **1** and **2** at the NMR timescale. Cross-peaks in $^{31}\text{P}/^{31}\text{P}$ EXSY experiments indicate that there is some chemical exchange, but it is slow at the NMR time-scale, no coalescence and even no broadening of the NMR signals being observed upon heating at 45°C (*SI Appendix*). The gold complex **2** behaves very differently than the corresponding anilinium salt

PhNMe₂H,OTf for which proton exchange between the base and acid forms is fast by NMR at room temperature and even at low temperature (a unique set of ¹H NMR signals is observed for the two species down to -70°C).

Computational studies of the cationic gold complex 2: geometry optimization and bonding analysis

A comprehensive theoretical study was performed to analyse the bonding situation in the gold complex **2** (*SI Appendix*). The main objective of these quantum chemical calculations was to establish unambiguously the presence of an attractive N-H...Au interaction and to precise its nature.

Geometry optimization. The B3PW91/SDD+f(Au),6-31G** (other atoms) level of theory was used and solvent effects (CH₂Cl₂) were taken into account by means of the continuum standard solvation SMD model. Calculations were first carried out on the naked cations. Several minima were located on the potential energy surface (Fig. 2, Table 1 and *SI Appendix*, Table S2). The ground-state structure **2a** parallels that observed by X-ray diffraction, with the N-H bond pointing towards Au. Two other *minima* **2b** and **2c** correspond to conformers associated with rotations around the C_{Ph}-N and C_{Ph}-P bonds. Another local *minimum* is the square-planar gold(III) hydride **2d**, in which the N center is coordinated to gold. **2d** results from oxidative addition of the N-H bond to gold and is reminiscent of the gold(III) pincer hydride complex recently reported by Bezuidenhout *et al* (42). In **2a**, the H atom at N enters the coordination sphere of gold (Au...H = 2.134 Å) with a quasi linear N-H...Au arrangement (174.2°), in line with that expected for hydrogen bonding. Comparison of the metrical data shows that the N-H bond is noticeably elongated upon interaction with gold (1.046 Å in **2a** versus 1.024-1.025 Å in **2b,c**). The conformers **2b** and **2c** are located 11-12 kcal/mol higher in energy than **2a**, which suggests some stabilization of **2a** thanks to N-H...Au interaction. The gold(III) hydride **2d** is even higher in energy, about 21 kcal/mol above **2a**. Inclusion of TfO⁻ in the calculations induces only small changes in the optimized geometries and relative energies of the gold(I) conformers, indicating that the counteranion has little influence (*SI Appendix*, Table S4). Relativistic effects are known to profoundly influence the properties of gold (5, 24, 43). To assess their impact on the gold-ammonium interaction in **2a**, ADF calculations were performed at the COSMO(DCM)-BP86/TZ2P//B3PW91/SDD+f(Au),6-31G** (other atoms) level of theory. When relativistic effects were not taken into account for the geometry optimization (calculation carried out without ZORA) the N-H bond departs from Au and strengthens (*SI Appendix*, Table S3), reflecting their importance in the structure of **2a**. In turn, this shows that the N-H...Au interaction is assisted by chelation but not imposed geometrically in **2a**.

<Fig. 2, Table 1>

Spectroscopic data. The ¹H NMR chemical shifts and IR stretching frequencies computed for the three gold(I) conformers **2a-c** corroborate the experimental assignment and confirm the presence of a N-H...Au hydrogen bond interaction in **2a** (Table 1). Upon interaction with gold, the ¹H NMR resonance signal for the N-H moiety is predicted to shift from 5.6-6.3 ppm for **2b,c** to 11.9 ppm for **2a**, in good agreement with the signal observed at 10.9 ppm experimentally. The N-H stretches computed for **2b** and **2c** are very similar in energy to that of the anilinium PhNMe₂H⁺ (~ 3500 cm⁻¹), while that of **2a** is about 500 cm⁻¹ red-shifted, indicating substantial weakening of the N-H bond upon interaction with gold (24, 41). For completeness, the N-D stretch for the deuterium-labeled **2a-D** was also computed (2089 cm⁻¹). The obtained value matches quite well with that determined experimentally (2124 cm⁻¹).

Bonding analysis. The bonding situation in **2a** was then analysed using various methods. Natural Bond Orbital (NBO) analyses (*SI Appendix*, Table S6) substantiate the weakening of the N–H bond upon interaction with gold. The Wiberg Bond Index (WBI) of the N–H bond decreases from 0.71–0.73 in **2b,c** to 0.61 in **2a**, while the WBI for the Au···H interaction in **2a** is small but significant (0.124). In the meantime, the computed NPA charges show some charge transfer from the metal fragment to the ammonium moiety: the charge for the PAuCl fragment increases from 0.65–0.71 in **2b,c** to 0.76 in **2a**, while the charge for the NMe₂H fragment decreases from 0.66–0.68 in **2b,c** to 0.61 in **2a**. This charge transfer is also apparent from the electrostatic potential (ESP) maps. Side views of **2a** and **2b** are displayed in Fig. 3, left. The ammonium moiety is located in a positive (blue) area in both cases, but when H-bonded to gold, its charge is reduced and the surface is lighter.

<Fig. 3>

Besides this electrostatic component, the NBO analysis revealed some orbital contribution to the N–H···Au interaction. A weak donor-acceptor interaction (delocalization energy $\Delta E(2) = 12.8$ kcal/mol) between an occupied d(Au) orbital and the $\sigma^*(\text{N–H})$ orbital was found at the second-order perturbation theory (Fig. 3, right). This picture is consistent with a 3c–4e interaction, as inferred for H-bonded complexes and as opposed to the 3c–2e interaction involved in agostic complexes (1, 44).

We then turned to Atom-In-Molecules (AIM) analysis. This electron density-based theoretical method is very powerful to analyse chemical bonding, including weak interactions. It has been recently complemented with NCI plots to detect, visualize and authenticate non-covalent interactions, in particular H-bonds (45). These methods have been used to probe and actually support theoretically the possibility for water to form H-bonds with anionic and neutral gold(I) complexes (22). The electron density at the N–H bond critical point (BCP) is smaller for **2a** than for the two conformers **2b,c** ($\rho = 0.319$ versus 0.343 e.bohr^{–3}), in line with the bond weakening delineated by IR and NBO. In addition, the ground-state structure shows a BCP between the Au and H atoms with $\rho = 0.039$ e.bohr^{–3} (see Fig. 4, left for the Laplacian of the electron density map). The Laplacian is positive (0.068 e.bohr^{–3}) and the second Hessian eigenvalue λ_2 is negative (-0.046), in line with bonding non-covalent Au···H interaction. This picture is corroborated by the NCI plot (Fig. 4, right). The large and negative value of $\text{sign}(\lambda_2)\rho$ between Au and H is indicative of attractive non-covalent interaction and consistent with N–H···Au hydrogen bonding (45).

<Fig. 4>

This detailed analysis thus provides compelling evidence for the presence of N–H···Au hydrogen bonding in **2a**. The computational methods and obtained results complete each other and are all consistent with a 3c–4e attractive interaction. Most diagnostic are the Au→NH⁺ transfer of electron density and the weakening of the N–H bond.

Generalization: preparation, bonding analysis of other gold(I) complexes.

To complete the study, we then aimed to generalize the bonding situation of **2a** to other gold complexes. First, we turned to the MorDalPhos ligand **5** with a morpholine instead of dimethylamine group next to phosphorus. The corresponding cationic gold complex **6** (Fig. 5) was prepared and characterized by multi-nuclear NMR spectroscopy (*SI Appendix*). Exchange of the TfO counteranion for the tetraarylborate BAr^{F}_4 ($\text{Ar}^{\text{F}} = 3,5\text{-(F}_3\text{C)}_2\text{C}_6\text{H}_3$) enables to grow crystals suitable for X-ray diffraction analysis. The proton at N resonates at low field in ^1H NMR (11.4 ppm). As apparent from the X-ray structure (*SI Appendix*), complex **6** adopts the same conformation than **2**. The N–H bond points towards Au (with a quasi-linear N–H \cdots Au arrangement, $174(8)^\circ$) and the H \cdots Au distance is quite short ($2.27(2)$ Å). DFT Calculations (*SI Appendix*) support further the analogy between **2** and **6**. The ground-state structure of the MorDalPhos complex **6** is that observed experimentally. Its geometric and spectroscopic features are very similar to those of **2** (*SI Appendix*, Table S5). Bonding analysis indicates the presence of Au \cdots H–N hydrogen bonding, whose magnitude is slightly weaker than for the MeDalPhos complex **2** according to NBO and AIM analyses (cf the numerical values of the WBI, NPA charges, second-order NBO delocalization energies, electron density at BCPs, *SI Appendix*, Table S6).

In addition, a couple of gold(I) complexes susceptible to display Au \cdots H hydrogen bonding were identified from recent literature (Fig. 5). Complex **7** was characterized by NMR and considered, but ruled out, as intermediate in the formation of a pincer Au(III) hydride complex (42). Complex **8** was envisioned as possible subunit in the assessment of aurophilic binding energies in the gas phase by mass spectrometry, without further identification of Au \cdots H–N hydrogen-bonding attractive interaction (41). According to the optimized geometries (*SI Appendix*), the H atom at N enters the coordination sphere of Au in both cases, with computed H \cdots Au distance of 2.22 and 2.45 Å, respectively. NBO and AIM analyses do support the presence of some H-type bonding (*SI Appendix*), albeit substantially weaker than those observed in the (P,NH $^+$) gold complexes derived from the Me and MorDalPhos ligands.

<Fig. 5>

Conclusion

By simple protonation of a ditopic (P,N) ligand, the cationic complex **2** featuring short contact between the gold(I) center and the proximal NH $^+$ ammonium moiety has been prepared. The presence of Au \cdots H–N hydrogen-bonding has been delineated experimentally by NMR, IR and XRD. The bonding situation has been confirmed and further assessed computationally. Geometry optimization, exploration of the potential energy surface and thorough analysis of the Au \cdots H–N interaction have provided compelling evidence for non-covalent attractive hydrogen-type bonding. Similar situations have been authenticated in other gold(I) complexes, demonstrating that **2** is not a unique case.

The hydrogen bonding evidenced here represents a new type of gold-hydrogen interaction, complementary to covalent Au–H bonds (gold hydrides) (42, 46–49) and Au \cdots H–C agostic interactions (50, 51) which have been recently authenticated and attract much interest (Fig. 6). This work contributes to advance further our knowledge of gold chemistry, which, despite recent advances (12, 52–57), remains far behind that of the other transition metals, in terms of structures as well as reactivity.

<Fig. 6>

Methods and data

Experimental procedures, analytical data including NMR spectra, crystallographic and computational details (including the Cartesian coordinates of the computed structures) are provided as Supporting Information. The crystallographic data including atom coordinates and structure factors have been deposited in the Cambridge Structural Database (CCDC 1868951-1868953) and can be obtained free of charge.

Acknowledgments

This work was supported financially by the Centre National de la Recherche Scientifique and the Université de Toulouse. UPPA (Université de Pau et des Pays de l'Adour), MCIA (Mésocentre de Calcul Intensif Aquitain) and CINES (Centre Informatique National de l'Enseignement Supérieur) under allocation A003080045 made by Grand Equipement National de Calcul Intensif (GENCI) are acknowledged for computational facilities. E. D. Sosa Carrizo thanks CDAPP for funding part of his post-doctoral contract.

References

1. Brammer L (2003) Metals and hydrogen bonds. *Dalton Trans* 3145–3157.
2. Martín A (1999) Hydrogen Bonds Involving Transition Metal Centers Acting As Proton Acceptors. *J Chem Educ* 76:578–583.
3. Kazarian SG, Hamley PA, Poliakoff M (1993) Is intermolecular hydrogen-bonding to uncharged metal centers of organometallic compounds widespread in solution? A spectroscopic investigation in hydrocarbon, noble gas, and supercritical fluid solutions of the interaction between fluoro alcohols and $(\eta^5\text{-C}_5\text{R}_5)\text{ML}_2$ (R = H, Me; M = Co, Rh, Ir; L = CO, C₂H₄, N₂, PMe₃) and its relevance to protonation. *J Am Chem Soc* 115:9069–9079.
4. Vedernikov AN, Caulton KG (2003) N–Pt^{IV}–H/N–H \cdots Pt^{II} intramolecular redox equilibrium in a product of H–C(sp²) cleavage and unusual alkane/arene C–H bond selectivity of ([2.1.1]pyridinophane)Pt^{II}(CH₃)⁺. *Chem Commun* 358–359.
5. Gorin DJ, Toste FD (2007) Relativistic effects in homogeneous gold catalysis. *Nature* 446:395–403.
6. Pyykkö P (2004) Theoretical Chemistry of Gold. *Angew Chem Int Ed* 43:4412–4456.
7. Hashmi ASK, Hutchings GJ (2006) Gold Catalysis. *Angew Chem Int Ed* 45:7896–7936.
8. Hashmi ASK, Toste DF (2012) *Modern Gold Catalyzed Synthesis* (Wiley-VCH, Weinheim).
9. Toste FD, Michelet V (2014) *Gold Catalysis: An Homogeneous Approach* (Imperial College Press).
10. Hutchings GJ (2018) Heterogeneous Gold Catalysis. *ACS Cent Sci* 4:1095–1101.
11. Ciriminna R, Falletta E, Della Pina C, Teles JH, Pagliaro M (2016) Industrial Applications of Gold Catalysis. *Angew Chem Int Ed* 55:14210–14217.
12. Schmidbaur H, Raubenheimer HG, Dobrzańska L (2013) The gold–hydrogen bond, Au–H, and the hydrogen bond to gold, Au \cdots H–X. *Chem Soc Rev* 43:345–380.

13. Nuss H, Jansen M (2006) [Rb([18]crown-6)(NH₃)₃]Au·NH₃: Gold as Acceptor in N–H···Au[−] Hydrogen Bonds. *Angew Chem Int Ed* 45:4369–4371.
14. Lusi M, Barbour LJ (2011) Determining Hydrogen Atom Positions for Hydrogen Bonded Interactions: A Distance-Dependent Neutron-Normalized Method. *Cryst Growth Des* 11:5515–5521.
15. Kraus F, Schmidbaur H, Al-juaid SS (2013) Tracing Hydrogen Bonding Au···H–C at Gold Atoms: A Case Study. *Inorg Chem* 52:9669–9674.
16. Schaper L-A, et al. (2013) Gold(I) Complexes with “Normal” 1,2,3-Triazolylidene Ligands: Synthesis and Catalytic Properties. *Organometallics* 32:3376–3384.
17. Koskinen L, Jääskeläinen S, Kalenius E, Hirva P, Haukka M (2014) Role of C–H···Au and Aurophilic Supramolecular Interactions in Gold–Thione Complexes. *Cryst Growth Des* 14:1989–1997.
18. Bakar MA, Sugiuchi M, Iwasaki M, Shichibu Y, Konishi K (2017) Hydrogen bonds to Au atoms in coordinated gold clusters. *Nat Commun* 8:576.
19. Kryachko ES, Karpfen A, Remacle F (2005) Nonconventional Hydrogen Bonding between Clusters of Gold and Hydrogen Fluoride. *J Phys Chem A* 109:7309–7318.
20. Kryachko ES, Remacle F (2007) The gold-ammonia bonding patterns of neutral and charged complexes Au_m^{0±1}–(NH₃)_n. I. Bonding and charge alternation. *J Chem Phys* 127:194305.
21. Kryachko ES (2008) Where gold meets a hydrogen bond? *J Mol Struct* 880:23–30.
22. Groenewald F, Dillen J, Raubenheimer HG, Esterhuysen C (2016) Preparing Gold(I) for Interactions with Proton Donors: The Elusive [Au]···HO Hydrogen Bond. *Angew Chem Int Ed* 55:1694–1698.
23. Groenewald F, Raubenheimer HG, Dillen J, Esterhuysen C (2017) Gold setting the “gold standard” among transition metals as a hydrogen bond acceptor – a theoretical investigation. *Dalton Trans* 46:4960–4967.
24. Berger RJF, Schoiber J, Monkowius U (2017) A Relativity Enhanced, Medium-Strong Au(I)···H–N Hydrogen Bond in a Protonated Phenylpyridine-Gold(I) Thiolate. *Inorg Chem* 56:956–961.
25. Schmidbaur H, Schier A (2011) Aurophilic interactions as a subject of current research: an update. *Chem Soc Rev* 41:370–412.
26. Sen S, Gabbaï FP (2017) An ambiphilic phosphine/H-bond donor ligand and its application to the gold mediated cyclization of propargylamides. *Chem Commun* 53:13356–13358.
27. Zheng Z, Wang Z, Wang Y, Zhang L (2016) Au-Catalysed oxidative cyclisation. *Chem Soc Rev* 45:4448–4458.
28. Luo Y, Ji K, Li Y, Zhang L (2012) Tempering the Reactivities of Postulated α-Oxo Gold Carbenes Using Bidentate Ligands: Implication of Tricoordinated Gold Intermediates and the Development of an Expedient Bimolecular Assembly of 2,4-Disubstituted Oxazoles. *J Am Chem Soc* 134:17412–17415.

29. Ji K, Zhao Y, Zhang L (2013) Optimizing P,N-Bidentate Ligands for Oxidative Gold Catalysis: Efficient Intermolecular Trapping of α -Oxo Gold Carbenes by Carboxylic Acids. *Angew Chem Int Ed* 52:6508–6512.
30. Ji K, Zheng Z, Wang Z, Zhang L (2015) Enantioselective Oxidative Gold Catalysis Enabled by a Designed Chiral P,N-Bidentate Ligand. *Angew Chem Int Ed* 54:1245–1249.
31. Wang Y, Zheng Z, Zhang L (2015) Intramolecular Insertions into Unactivated C(sp³)–H Bonds by Oxidatively Generated β -Diketone- α -Gold Carbenes: Synthesis of Cyclopentanones. *J Am Chem Soc* 137:5316–5319.
32. Zeineddine A, et al. (2018) Isolation of a Reactive Tricoordinate α -Oxo Gold Carbene Complex. *Angew Chem Int Ed* 57:1306–1310.
33. Zeineddine A, et al. (2017) Rational development of catalytic Au(I)/Au(III) arylation involving mild oxidative addition of aryl halides. *Nat Commun* 8:565.
34. Bontemps S, Bouhadir G, Miqueu K, Bourissou D (2006) On the Versatile and Unusual Coordination Behavior of Ambiphilic Ligands o-R₂P(Ph)BR'₂. *J Am Chem Soc* 128:12056–12057.
35. Amgoune A, Bourissou D (2010) σ -Acceptor, Z-type ligands for transition metals. *Chem Commun* 47:859–871.
36. Devillard M, et al. (2015) Dative Au→Al Interactions: Crystallographic Characterization and Computational Analysis. *Chem – Eur J* 21:74–79.
37. Batsanov SS (2001) Van der Waals Radii of Elements. *Inorg Mater* 37:871–885.
38. Zhang Y, Lewis JC, Bergman RG, Ellman JA, Oldfield E (2006) NMR Shifts, Orbitals, and M···H–X Bonding in d⁸ Square Planar Metal Complexes. *Organometallics* 25:3515–3519.
39. Pregosin PS, et al. (1992) New P···H–N bonds characterized by ¹⁵N-filtered and 2D NOESY ¹H NMR spectroscopy. *Magn Reson Chem* 30:548–551.
40. Wehman-Ooyevaar ICM, et al. (1992) A hydrogen atom in an organoplatinum-amine system. 1. Synthesis and spectroscopic and crystallographic characterization of novel zwitterionic complexes with a Pt(II)···H–N⁺ unit. *J Am Chem Soc* 114:9916–9924.
41. Andris E, et al. (2018) Aurophilic Interactions in [(L)AuCl]···[(L')AuCl] Dimers: Calibration by Experiment and Theory. *J Am Chem Soc* 140:2316–2325.
42. Kleinhans G, et al. (2016) Nucleophilic T-Shaped (LXL)Au(I)-Pincer Complexes: Protonation and Alkylation. *J Am Chem Soc* 138:15873–15876.
43. Jerabek P, Vondung L, Schwerdtfeger P (2018) Tipping the Balance between Ligand and Metal Protonation due to Relativistic Effects: Unusually High Proton Affinity in Gold(I) Pincer Complexes. *Chem – Eur J* 24:6047–6051.
44. Yao W, Eisenstein O, Crabtree RH (1997) Interactions between C–H and N–H bonds and d⁸ square planar metal complexes: hydrogen bonded or agostic? *Inorganica Chim Acta* 254:105–111.

45. Johnson ER, et al. (2010) Revealing Noncovalent Interactions. *J Am Chem Soc* 132:6498–6506.
46. Tsui EY, Müller P, Sadighi JP (2008) Reactions of a Stable Monomeric Gold(I) Hydride Complex. *Angew Chem Int Ed* 47:8937–8940.
47. Roşca D-A, Smith DA, Hughes DL, Bochmann M (2012) A Thermally Stable Gold(III) Hydride: Synthesis, Reactivity, and Reductive Condensation as a Route to Gold(II) Complexes. *Angew Chem Int Ed* 51:10643–10646.
48. Pintus A, Rocchigiani L, Fernandez-Cestau J, Budzelaar PHM, Bochmann M (2016) Stereo- and Regioselective Alkyne Hydrometallation with Gold(III) Hydrides. *Angew Chem Int Ed* 55:12321–12324.
49. Rocchigiani L, Fernandez-Cestau J, Chambrier I, Hrobárik P, Bochmann M (2018) Unlocking Structural Diversity in Gold(III) Hydrides: Unexpected Interplay of cis/trans-Influence on Stability, Insertion Chemistry, and NMR Chemical Shifts. *J Am Chem Soc* 140:8287–8302.
50. Rekhroukh F, et al. Experimental and Theoretical Evidence for an Agostic Interaction in a Gold(III) Complex. *Angew Chem Int Ed* 55:3414–3418.
51. Rekhroukh F, et al. (2016) β -Hydride Elimination at Low-Coordinate Gold(III) Centers. *J Am Chem Soc* 138:11920–11929.
52. Heinze K (2017) The Quest for Mononuclear Gold(II) and Its Potential Role in Photocatalysis and Drug Action. *Angew Chem Int Ed* 56:16126–16134.
53. Hashmi ASK (2012) Fire and Ice: A Gold(III) Monohydride. *Angew Chem Int Ed* 51:12935–12936.
54. Teles JH (2015) Oxidative Addition to Gold(I): A New Avenue in Homogeneous Catalysis with Au. *Angew Chem Int Ed* 54:5556–5558.
55. Joost M, Amgoune A, Bourissou D (2015) Reactivity of Gold Complexes towards Elementary Organometallic Reactions. *Angew Chem Int Ed* 54:15022–15045.
56. Benitez D, et al. (2009) A bonding model for gold(I) carbene complexes. *Nat Chem* 1:482–486.
57. Wang Y, Muratore ME, Echavarren AM (2015) Gold Carbene or Carbenoid: Is There a Difference? *Chem – Eur J* 21:7332–7339.

Figures & Table Captions

Fig. 1. Gold complexes deriving from chelating (P,N) and ambiphilic (P,E₁₃) ligands.

Scheme 1. Synthesis (two routes) and X-ray structure of the (P,NH⁺) gold(I) complex **2** derived from MeDalPhos. Thermal ellipsoids are drawn at 50% probability, the TfO⁻ counter-anion and hydrogen atoms, except that on nitrogen, are omitted for clarity. Selected bond lengths (Å) and bond angles (°): P–Au 2.270(1), Au–Cl 2.283(1), Au⋯H 2.24(3), P–Au–Cl 176.98(2), N–H⋯Au 165(2).

Fig. 2. Energy minima located on the potential energy surface of complex **2**. Relative energies in kcal/mol (ΔG values, with ΔE values into brackets).

Table 1. Key geometric features (distances in Å, angles in °) and spectroscopic data for the three conformers **2a-c**.

Fig. 3. Left: Electrostatic potential maps for **2a** (with the N–H bond pointing and hydrogen-bonded towards Au) and **2b** (with the N–H bond pointing opposite to gold) plotted over the range 0.1 (red) to 0.3 au (blue). The isosurfaces are drawn at 0.002 e.au⁻³. Right: Superposition of the donor and acceptor NBO orbitals (cutoff = 0.08) involved in the N–H⋯Au interaction. Participation of each atom in percent in the associated NLMO.

Fig. 4. Left: Contour plot of the Laplacian distribution $\nabla^2\rho(r_c)$ for **2a** with relevant bond paths and bond critical points (green spheres). Hydrogen atoms have been omitted for clarity except that on the nitrogen atom. Right: NCI plot for **2a**. Gradient isosurface ($s = 0.5$ au) colored according to a BGR scheme over the range of $-0.05 < \text{sign}(\lambda_2)\rho < 0.05$ au. Blue indicates strong attraction, green indicates very weak interaction, and red indicates strong repulsion.

Fig. 5. Chemdraw structures, optimized geometries (distances in Å, angles in °) and calculated electron density maps (Laplacian plot) of the gold(I) complexes **6**, **7** and **8**.

Fig. 6. Different types of molecular gold complexes featuring Au⋯H interactions authenticated so far (selected examples for gold(III) hydrides).

Figures & Table

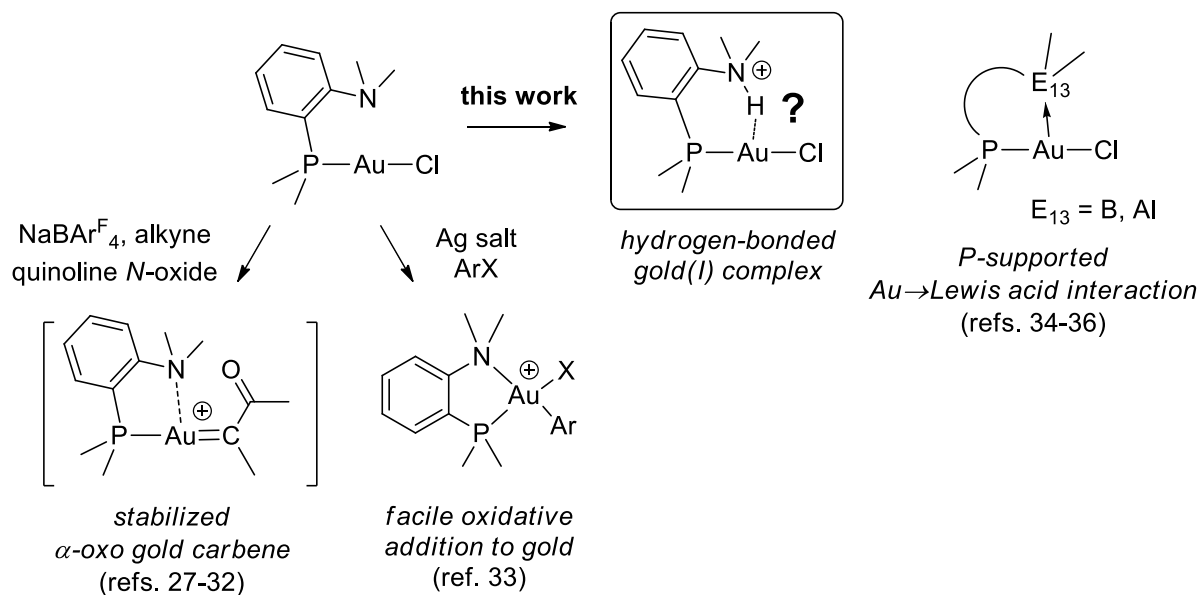
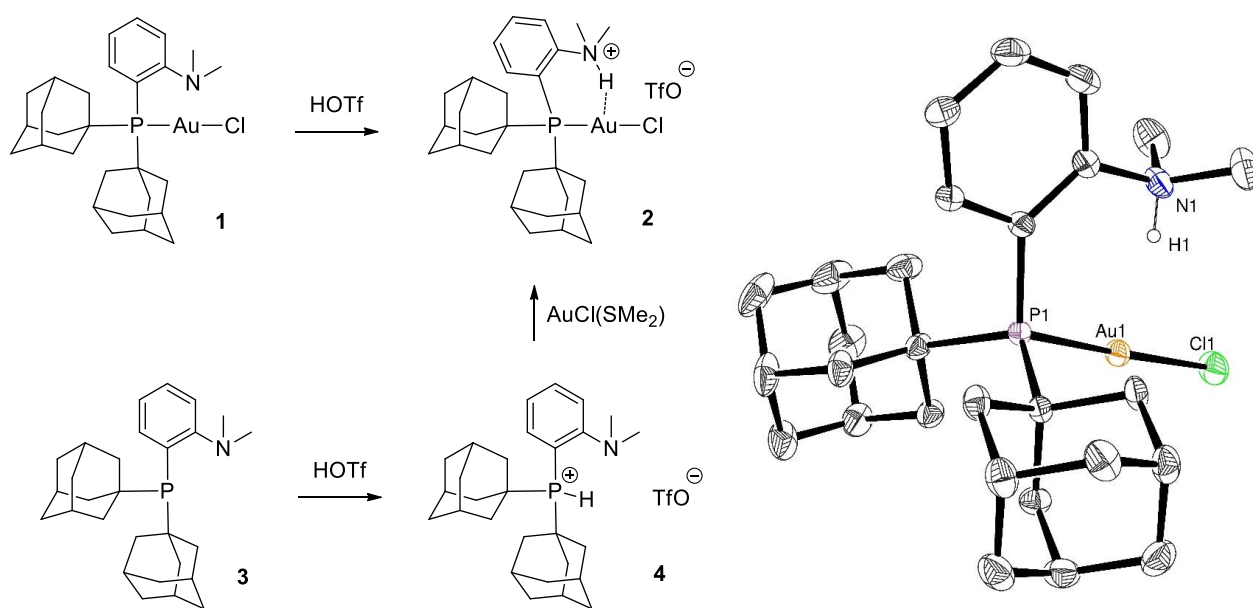


Fig. 1.



Scheme 1.

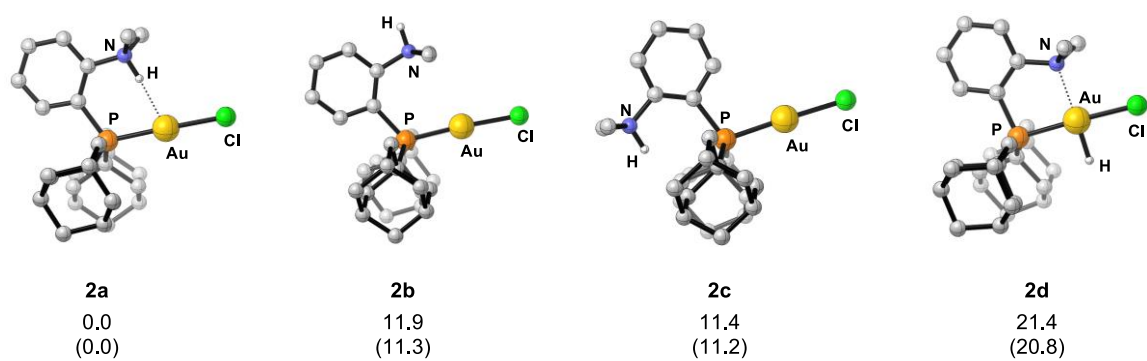


Fig. 2.

Table 1.

	2a	2b	2c
P–Au	2.303	2.304	2.305
Au–Cl	2.338	2.344	2.339
N–H	1.046	1.024	1.025
Au···H	2.134	/	/
P–Au–Cl	178.53	176.51	178.14
N–H···Au	174.18	/	/
ν_{NH} (cm^{-1})	3032.27	3457.31	3445.89
$\Delta\nu_{\text{NH}}$ with HNMe_2Ph^+	-443.32	-18.28	-29.7
$\delta^1\text{H}$ NMR (NH, ppm)	11.94	5.64	6.31

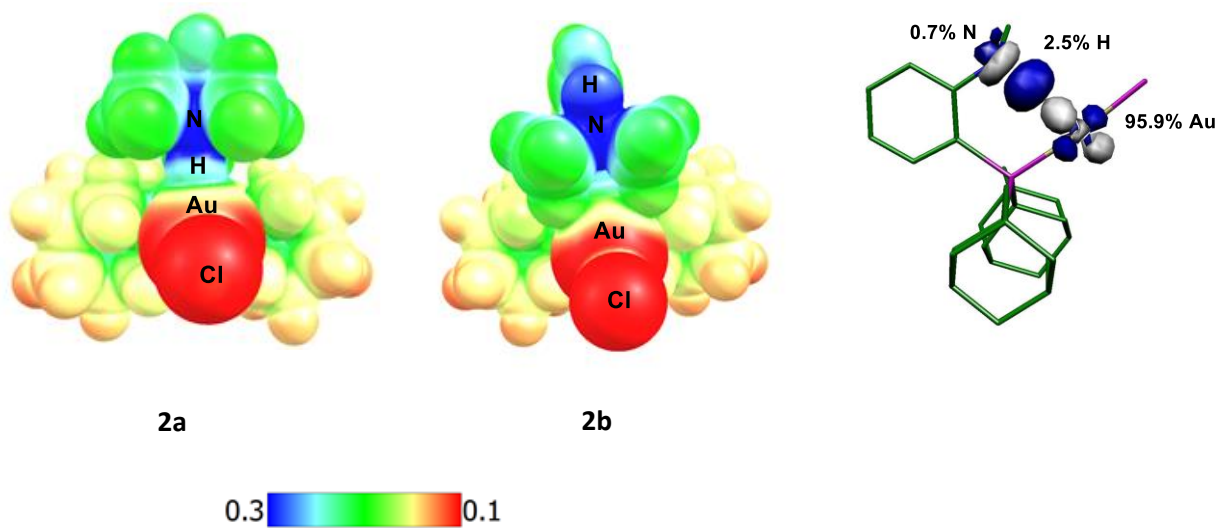


Fig. 3.

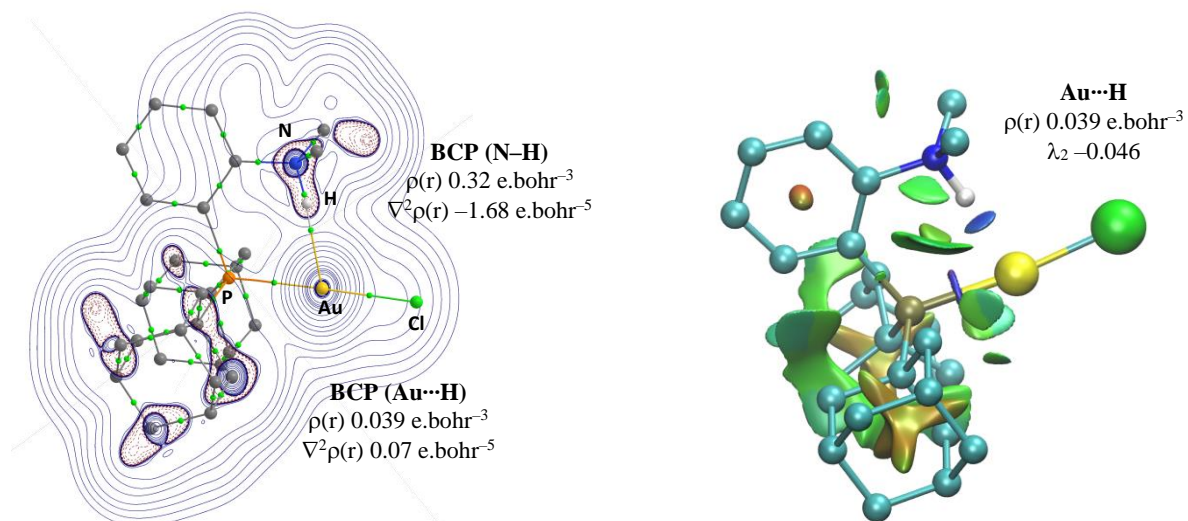


Fig. 4.

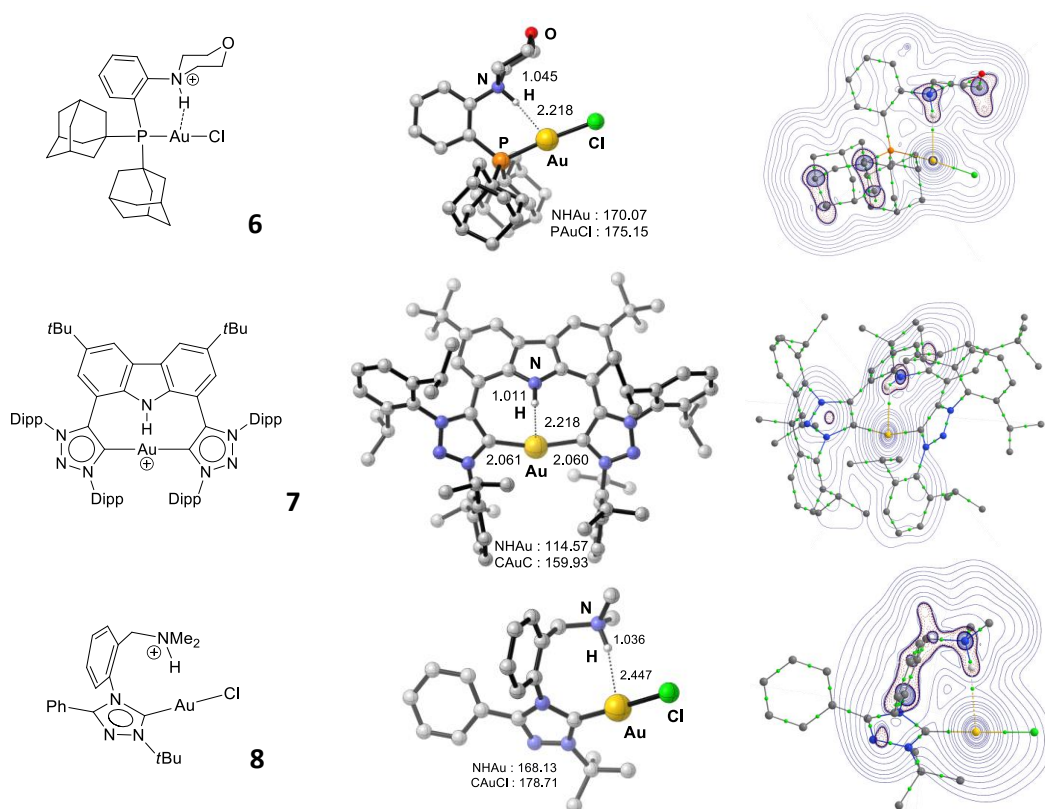


Fig. 5.

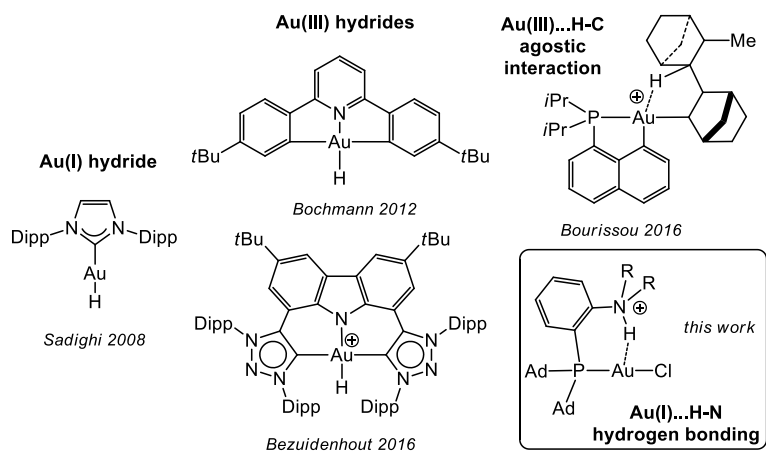


Fig. 6.